INNOVATION

ORIGINAL ARTICLE

Mechanism of Cortical Bone Adaptation to Static Forces

Alikhani M [a,b], Alikhani M [a], Sangsuwon C [a], Oliveira SP [a,c], Abdullah F [a], Teixeira CC [d]

a *CTOR Academy, Hoboken, New Jersey*

b *Harvard University, Department of Developmental Biology, Boston, Massachusetts*

c *CISeD Research Center in Digital Services, Polytechnic University of Viseu, Portugal*

d *New York University, Department of Orthodontics, New York, New York*

Corresponding Author:
Cristina Teixeira
345 East 24th Street
New York, NY 10010
Tel (212) 998-9224
Fax (212) 995 4087
Cristina.Teixeira@nyu.edu

Citation: *Alikhani, M., Alikhani, M., Sangsuwon, C. Oliveira, SP. Abdullah, F. & Teixeira, CC. "Mechanism of Cortical Bone Adaptation to Static Forces." Innovation, February 2024, 2(2),1-16. https://doi.org/10.30771/2024.2*

Submitted February 1, 2024
Accepted February 29, 2024

Keywords: *Periosteum, Endosteum, Inflammation, Expansion, Constriction, Osteoclasts, Tensile stress, Compressive stress, Sutures, Maxilla, Osteoblasts, Orthopedic, Inflammatory Markers, Mechanical Stimulation, Bone formation, Static, Dynamic, Forces*

Abstract

The mechanism of cortical bone adaptation to static forces is not well understood. This is an important process since static forces are applied to cortical bone in response to growth of soft tissues or any pathologic changes in the size or position of soft tissues. In addition, static forces are applied during Orthodontic and Orthopedic corrections.

Materials & Methods: 375 adult Sprague-Dawley rats were divided into four groups: 1) control group that did not receive any appliance or force, 2) static force group that received 50 cN static force applied to the hemimaxilla, 3) static force plus stimulation group that received static force plus periosteal stimulation, 4) sham group that received the same appliance as the static force group without any force application or periosteal stimulation. In addition to static force, some animals were exposed to anti-inflammatory medication. Samples were collected at 0, 1, 3, 7, 14, 28 and 56 days, and evaluated by micro-computed tomography, fluorescence microscopy, immunohistochemistry, and gene and protein analyses.

Results: The application of static forces to the hemimaxilla induced the release of inflammatory markers in the periosteum followed by osteoclast activation. This activation was independent of the increase in the convexity of the bone or the magnitude of tooth movement, but followed the pattern of skeletal displacement. Bone formation on the surface of cortical plate occurred a later stage and resulted in relocation of the cortical boundary of the maxilla, cortical drifting.

Conclusion: This study demonstrates that cortical bone adaptation to static forces originates from the periosteum and not the bone itself, and it is an inflammatory-based phenomenon that can be manipulated by the clinician.

Innovation: Our findings are novel and, for the first time, support a new theory for cortical adaptation to static forces. This work is critical for understanding the effect of static physiologic or pathological forces on cortical bone, such as those resulting from growth or chronically expanding cysts and tumors. In addition, these results support an innovative clinical approach to promote cortical drifting through periosteal stimulation. Being able to control cortical drift can have a significantly impact in clinical orthodontic and dentofacial orthopedics by allowing corrections of severe deformities without need for maxillofacial surgery.

Introduction

It has been shown that trabecular bone can sense dynamic forces. In response to low-magnitude dynamic forces, quick changes in trabecular density give the skeleton a fast adaptation ability [1, 2]. Similarly, cortical bone demonstrates sensitivity to dynamic forces however, in comparison with trabecular bone, the changes in cortical bone take place over a longer period of time and are initiated in response to higher dynamic forces [3-6]. These characteristics make cortical bone the prominent load-bearing bone in our skeleton [7].

Interestingly, neither trabecular nor cortical bones show sensitivity to static forces [2, 4, 8, 9], which can explain why lack of activity can cause trabecular bone loss even when the static force of gravity is present [10]. Likewise, the application of static orthodontic forces to implants does not stimulate cortical bone response around the implant [11].

Previously, we and others have demonstrated that the mechanism of trabecular bone and cortical bone adaptation to dynamic forces originated either indirectly from strain-induced-changes in the matrix recognized by the bone cells [12-17] or by direct recognition of this mechanical stimulation by the cells themselves [2, 18]. Signals produced by static forces are too short in duration to be able to stimulate bone cells directly or indirectly, which could explain why both trabecular and cortical bone are not responsive to static forces [19, 20].

While static forces are not osteogenic, in many clinical scenarios, the application of static forces by a growing pathology could stimulate bone formation. For example, an increase in the size of a chronically growing cyst or tumor can cause bone formation [21-23]. Considering these pathologies grow very slowly, the force produced by these growing structures can be considered mostly static. While some experimental models show that static forces may modify the shape of the cortical bone [24, 25], those observations suggest that the target of static forces is not the bone itself.

Here, we investigate the response of the cortical bone of the jaws to a static force over a period of 56 days. Particularly, we studied the role of the periosteum on cortical bone adaptation to static forces and how we can harness periosteum response to stimulate cortical bone changes.

Materials and Methods

Animal Study

375 adult Spraque-Dawley rats (average body weight 360g, 120 days of age) were maintained following USA guidelines for laboratory animal housing. All animals were housed in polycarbonate cages in a 12-hour light/dark environment at the constant temperature of 23°C, and fed a standard pellet diet (Stepfield, Witham, Essex, UK) with tap water ad libitum. Animals were randomly divided into different groups and treated either with static force (different directions), static force plus periosteal stimulation (bilateral or unilateral), static force and anti-inflammatory medication, control (no appliance), or sham (appliance installed with no activation).

In some animals, the anti-inflammatory drug Diclofenac (5mg/kg) was injected intramuscularly (IM) daily with changing injection sites to prevent additional discomfort. Animals were weighed daily to calculate the dose of the medication for each animal accurately.

Bone labeling was performed using an intraperitoneal injection of Calcein green (15 mg/kg) on Days 0, 28 and 54 or Calcein green on day 0, and Xylenol Orange (90mg/kg) on days, 26 and 54. Animals were euthanized by CO2 narcosis on Days 0, 1, 3, 7, 14, 28, and 56.

Application of static force

On Day 0, animals were anesthetized with an intraperitoneal injection of Ketamine and Xylazine (0.09mL/ 100g). Anesthesia was verified by lack of response to toe-pinch. The static force was delivered by a calibrated custom-designed expanding spring that applied a 100 cN force to the molars. This force was selected based on previous studies demonstrating that 100cN induces cellular activity in maxillary sutures [26]. This force is not considered excessive, when compared with regular vertical chewing forces of the rats that, on average, are around 54-76 N [27].

Expanding springs were fabricated from 0.016” stainless steel wires (3M Unitek, Monrovia, CA, USA), bent into a single helix placed mesial to first molars while the arms engage around maxillary molars. (Figure 1A). The springs were secured with flowable resin around the molars. The springs were calibrated to produce 100 cN force (50 cN on each side) using a digital force gage (Figure 1B). The application of static forces was carried out for 56 Days, as noted above.

Animals and the integrity of the springs were monitored daily under inhalation anesthesia (isoflurane–nitrous oxide). If springs were dislodged, they were reinstalled at that time.

Periosteal Stimulation

Stimulation of the periosteum was accomplished with a custom designed appliance with two rows of 4 needles (Figure 1C). The stimulation was done in an area extending from the distal of first molar to the mesial of third molar (Figure 1D), bilaterally or unilaterally at day 0 and day 28.

Micro CT Imaging

The entire rat heads were collected and fixed for 72 hours with 4% (w/v) paraformaldehyde in 0.1 M phosphate buffer, pH 7.4 followed with storage in 70% ethanol. The samples were scanned in a Scanco MicroCT (µCT40, Scanco Medical AG, Bassersdorf, Switzerland). The skulls were scanned at an energy of 70 kV and intensity of 114 mA, with 300 ms integration time, resulting in a 16-mm isotropic voxel size. Results were analyzed utilizing µCT V6.0 software on the HP open platform (OpenVMS Alpha Version 1.3-1 session manager). Frontal

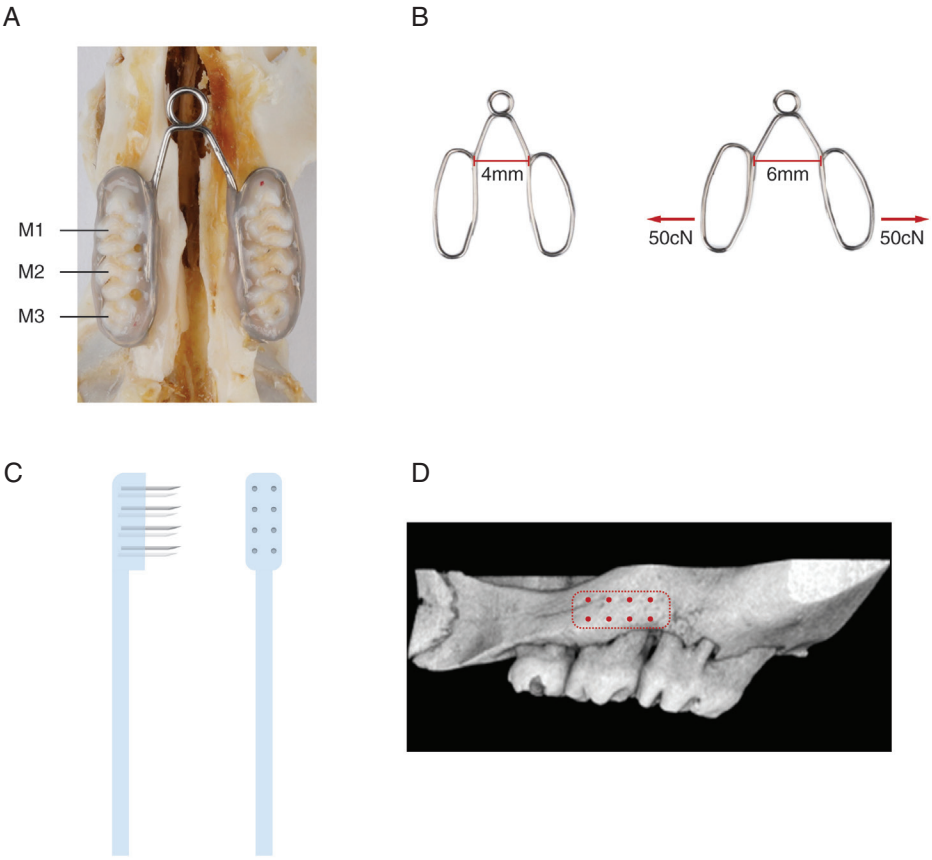

Figure 1: Schematic of model for application of static forces and periosteal stimulation. *Calibrated springs used to produce static forces on the rat maxilla were fabricated from 0.016" stainless steel wires (3M Unitek, Monrovia, CA, USA) and secured to teeth by flowable resin. Photograph of spring installed in the rat maxilla (A). The springs were calibrated using a digital force gage to produce 100cN force when expanded from 4 to 6 mm (B). Periosteum stimulation was performed using 8 needles attached to a handle (C). The device was used to produce small perforations in the periosteum. Perforations were applied in the area of buccal cortical plate of second molars (D). (M1 = first molar, M2 = second molar, M3= third molar).*

sections of the scanned maxilla were compared at the area of mesial roots of second molars.

The width of palate (distance between the palatal walls at the level of intersection between palate and alveolar bone wall) was measured in the micro CT images at the level of the mid-coronal plane of the maxillary second molar. The magnitude of unilateral tooth movement was calculated by subtracting palate width from the inter-dental width (distance between height of contour of second molars) and dividing the difference by two. Two examiners completed all quantifications.

Histology, Immunohistochemistry, and Fluorescence Microscopy

Maxillae were demineralized in 14% ethylenediaminetetraacetic acid (EDTA) for 3-4 weeks at 4°C, and dehydrated in ethanol gradients and xylene prior to embedding in paraffin. Sample embedded in paraffin was cut into 5 µm occlusal sections, using Leica Biosystems RM2265 Fully Automated Rotary Microtome. Five consecutive sections were used for TRAP staining.

For identification of osteoclasts, sections were immunostained using Vectastin ABC kit (Vectastin ABC kit, Vector Labroratories, Burlingame, CA, USA) with an antibody for tartrate-resistant acid phosphatase (TRAPcP-5b; Zymed antibodies; Invitrogen, Carlsbad, CA, USA), a marker of osteoclasts. As negative control, sections were exposed to pre-immune serum. Sections of each sample were scanned on a Scan Scope GL series optical microscope (Aperio, Bristol, UK) and analyzed at 20x magnification.

Osteoclasts were defined as TRAP-positive multinuclear cells on the surface of cortical bone of maxillary alveolar bone between the mesial border of the middle roots of the first molars and distal border of the distal roots of the second molars (Figure 2A). They were quantified as the mean of three measurements per section in the middle third of the occlusal section of maxillary alveolar bone in a fixed frame (3.5 mm x 0.5mm). Five animals were used for each group and two examiners completed all histological quantifications.

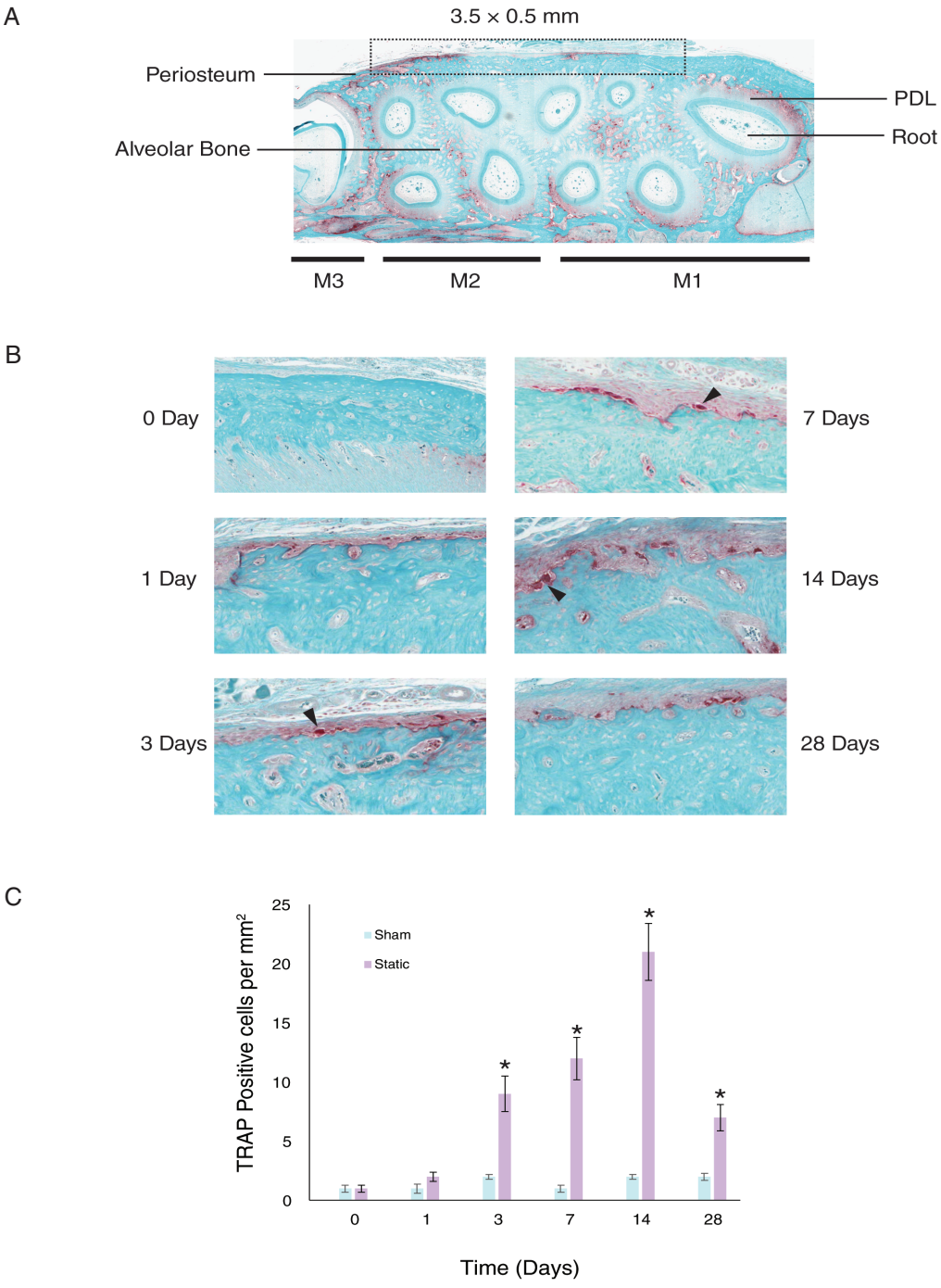

Figure 2: Static forces increase the number of osteoclasts in periosteum. *In response to application of 100cN static forces osteoclasts number and activity increased significantly in the periosteum of the buccal surface of alveolar bone. Immunohistochemistry for TRAP was performed in paraffin sections to identify active osteoclasts in the area shown in this image (A). Light microphotographs show TRAP-positive osteoclasts in the surface of cortical bone at different time points osteoclasts are stained as dark red cells (arrowheads in B, magnification 20X). Mean numbers of osteoclasts at different time points (B), were defined as TRAP-positive cells on the surface of cortical bone of maxillary alveolar bone between the mesial border of the mesial roots of the first molars and distal border of the distal roots of the second molars as shown in the dashed box in A. Each value represents the mean ± SD of five animals (C). *Static group significantly different from sham, p<0.05.*

For fluorescence microscopy, fixed specimens were, washed overnight in running water, dehydrated in an alcohol series, cleared with xylene, and embedded in methyl methacrylate according to the method of Erben [28]. Samples were sectioned at 5-µm thickness on a RM 2265 Leica microtome (Leica Biosystems, Buffalo Grove, IL, USA), viewed and photographed (Leica DMRX/E Universal Microscopy, Turboscan software, Cambridge, UK).

RNA Analysis

For total RNA extraction, 5 animals from each group were sacrificed at different time points by CO_2 narcosis at 24 hours, and the soft tissue surrounding the buccal surface of alveolar bone including periosteum was dissected and frozen in liquid nitrogen. After RNA extraction, Real-time PCR for bone formation and bone resorption markers was performed with primers specific for rat genes, with a QuantiTect SYBR Green RT-PCR kit (Qiagen, Valencia, CA) on a DNA Engine Optican 2 System (MJ Research, Waltham, MA). An mRNA pool for each group was tested three times. Relative levels of mRNA were calculated and normalized to the level of GAPDH and acidic ribosomal protein mRNA.

Protein Analysis

Levels of inflammatory markers were measured by enzyme-linked immunosorbent assay (ELISA). The soft tissue covering the buccal cortical plate of alveolar bone was dissected from 5 animals, frozen in liquid nitrogen, and pulverized. Lysates were prepared, and total protein was quantitated using a BCA protein assay kit (Pierce, Rockford, IL). Concentration of interleukin (IL)-1α (Thermo, Rockford, IL), tumor necrosis factor alpha (TNF-α) (Thermo, Rockford, IL), CCL5 (Abnova, Walnut, CA), and CCL2 (Abcam, Cambridge, MA), were determined by ELISA. Data were analyzed in comparison to standard curves specific to each inflammatory marker.

Sample size calculation and statistical analysis

The sample size was calculated based on the results of our previous animal studies, assuming an estimated 50% difference in the expression of inflammatory markers in periosteum Type I error was set at 5% and the power of the statistical test was set at 90% (power = 0.9, β=0.1). Based on this calculation, a sample size of 4 per group was suggested. We decided to increase the sample size to 5 to account for attrition.

After confirming the normal distribution of samples by the Shapiro-Wilk test, group comparisons were assessed by analysis of variance (ANOVA). Pairwise multiple comparison analysis was performed with Tukey's *post hoc* test. Two-tailed p values were calculated; $p < 0.05$ was set as the level of statistical significance.

RESULTS

Osteoclasts appear in periosteum in response to static forces

The health status and body weight of the rats were evaluated daily, and no significant differences were observed among groups. In response to application of transverse static forces, osteoclasts appeared in the buccal periosteum (Figure 2A). The number of osteoclasts increased overtime from day 1 to day 28, with a peak on day 14 (Figure 2B). The number of TRAP positive osteoclasts was measured in the surface of cortical bone at different time points in an area defined along the roots of first and second molars (Figure 2A). The increase in the number of osteoclasts in the static force group at day one was not statistically significant in comparison with sham group ($p>0.05$) (Figure 2C). However, the increase in osteoclast numbers was statistically significant for all other time points, when compared to sham group ($p<0.01$). By day 28 a trend towards a decrease in the number of osteoclasts was observed ($p<0.05$) (Figure 2C).

Osteoclasts appearance in the periosteum follows palatal width increase but precedes tooth movement

In response to static transverse forces across the maxilla the width of the palate increased and the molars moved laterally (Figure 3A). Palatal width increased significantly on day 3,7, 14 and 28, with the peak increase on day 14, which in comparison with sham group was statistically significant ($p<0.01$) (Figure 3B). The appearance of osteoclasts in the periosteum followed the pattern of increase in palatal width (compare Figure 2C with Figure 3B).

However, the appearance of osteoclast in the periosteum occurred ahead of tooth movement (compare Figure 2C with Figure 3C) and it was not related to magnitude of tooth movement. The magnitude of unilateral tooth movement in the experimental group in comparison with control group was statistically significant only on day 14 and 28 ($p< 001$) (Figure 3C). No significant amount of tooth movement was observed on day 1,3 and 7 and in none of the time points did the tooth movement reach the cortical plate (Figure 3D). In addition, the appearance of osteoclast in the periosteum was not limited to the area close to the teeth and could be observed further away, mesial to the molars area (Figure 3E).

Activation of osteoclast in periosteum was not due to increase in convexity of alveolar bone

To test if activation of osteoclasts in the periosteum is an attempt by alveolar bone to decrease the convexity induced by static forces, the direction of force was reversed (lingual direction). Application forces in both the buccal direction (increasing the convexity of alveolar bone) and lingual direction (decreasing the convexity of the alveolar bone) were able to activate osteoclasts in the periosteum (Figure 4A and

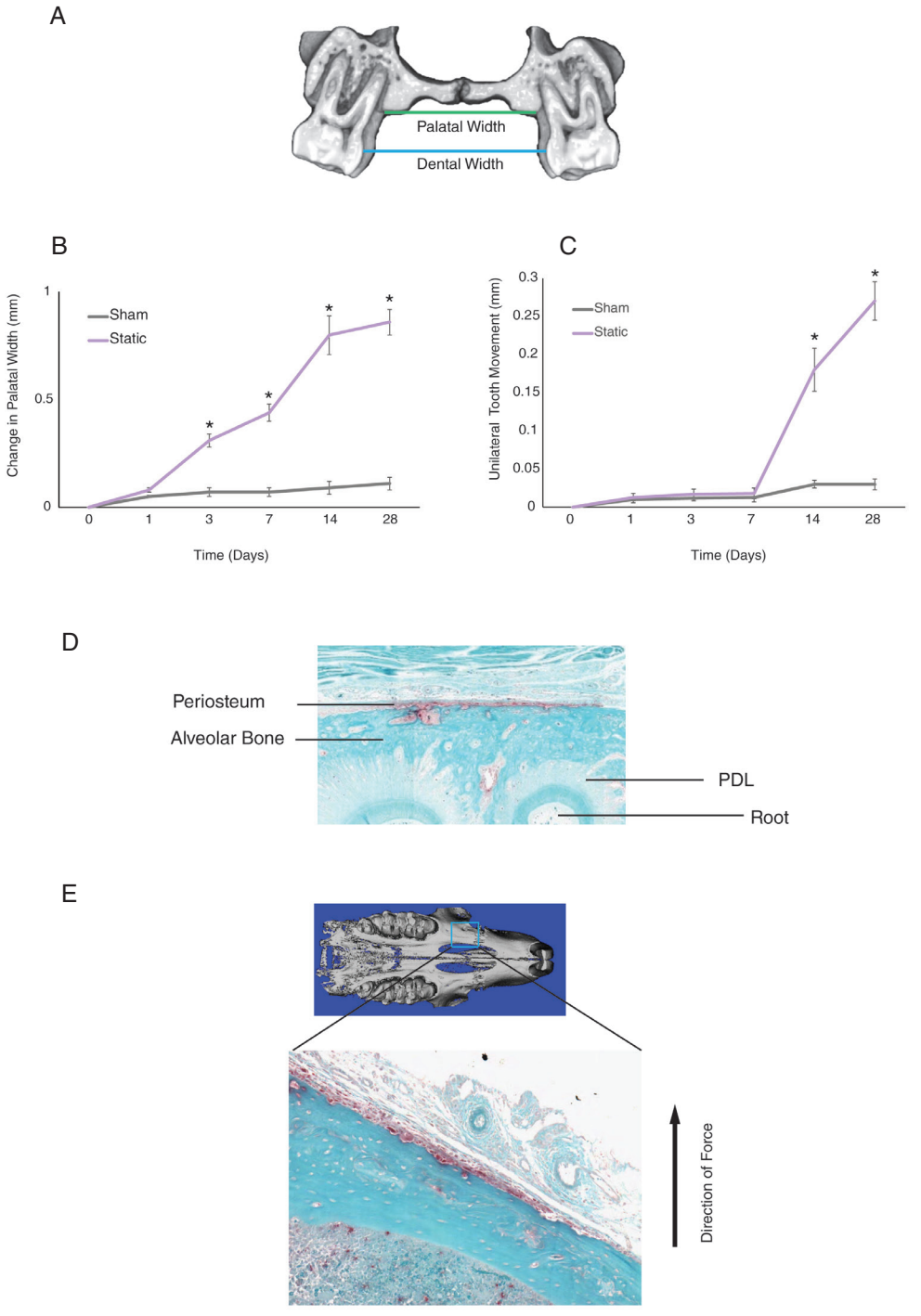

Figure 3: Increase in osteoclasts in periosteum follows palatal width increase but precedes tooth movement. *Palatal width and dental width of the maxilla were measured using micro CT 3D reconstructed images, and sections at the level of the mid-coronal plane of the maxillary second molar. Green line shows the width of palate (distance between the palatal walls at the level of intersection between palate and alveolar walls), and blue line shows the dental width (distance between height of contour of second molars) (A). The palatal widths were measured over time in both Static and Sham maxillae (B). Unilateral tooth movement was measured as described in Materials & Methods section at different time points (C). Data expressed as the mean ± SD of distances in mm. Each number represents the average of 5 samples. * Static group significantly different from sham, p<0.05. Histological section of periosteum in the area of second molar at day 7 shows osteoclasts activation in the periosteum ahead of tooth movement and before tooth reach the surface of cortical bone (D). Trap staining of the hemimaxilla in non-tooth bearing area midway between posterior teeth and anterior teeth demonstrates osteoclasts activation in periosteum and bone, in response to transverse forces applied to posterior teeth. Black arrows illustrate the direction of force (E).*

B). In addition, appearance of osteoclasts was not limited to periosteum but also observed in the endosteum (Figure 4C). Similar to periosteum, osteoclast appeared not only in the compression side but also in the tension side of periodontal ligament (PDL) (Figure 4B and C) suggesting activation of osteoclasts is not dependent on the bending of the bone nor the type of force (tension versus compression).

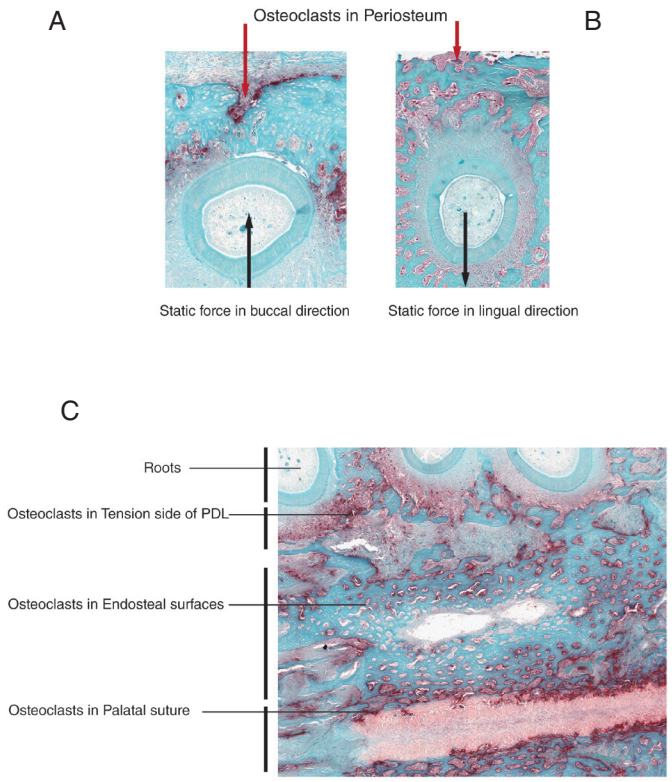

Figure 4: Activation of osteoclasts is independent of changes in convexity of the cortical bone. *100 cN static force was applied perpendicular to hemimaxilla expanding the palate (increasing the convexity in buccal cortical plate), or constricting the palate (decreasing the convexity of buccal cortical plate). Histological sections were taken in area of buccal cortical plate of second molar. TRAP staining was performed on 14 days sections to identify osteoclasts. Application of static forces toward the cortical plate and periosteum (A) or in opposite direction (B), both stimulate osteoclasts activation in the periosteum. Black arrows show the direction of the force. Application of 100cN static force to posterior teeth stimulate TRAP-positive cells not only in periosteum but also in endosteum (C). Section includes bone in the area of second molar extending from suture to lingual cortical plate. TRAP staining shows day 14 of the static group. Osteoclasts activation was observed in suture, endosteum of palate and in the tension side of PDL.*

Activation of osteoclasts is an inflammatory-based phenomenon.

The activation of osteoclasts in the periosteum occurred independently of the increase in convexity of the bone and was not related to tooth movement. We hypothesize that the change in alveolar bone position during buccal or lingual displacement in response to static forces, can traumatize the periosteum and therefore, the appearance of osteoclasts in the periosteum is a trauma-based phenomenon. To investigate this hypothesis, we studied the expression of inflammatory cytokines (IL-1β, TNFα) and chemokines (CCL-2 and CCL-5) in the soft tissue covering the buccal cortical plate 28 days after application of static forces (Figure 5A). This soft tissue included the buccal periosteum. Inflammatory markers were present in soft tissue at all time points during static force application and their expression was significantly higher in comparison with sham group ($p<0.05$). Levels of each cytokine and chemokine peaked twice in the periosteum, once on Day 1 and again on Day 14. This expression gradually decreased until day 28.

To demonstrate that inflammation is the signal stimulating osteoclasts activity in the periosteum, animals were exposed to similar static forces in presence or absence of anti-inflammatory medication. In the presence of anti-inflammatory medication, no osteoclast activity was observed in periosteum at day 7 (Figure 5B) even though the alveolar bone was exposed to static forces. To further demonstrate that trauma plays a significant role in osteoclast activation in the periosteum, a force was applied in the sagittal direction, parallel to the alveolar cortical plate and to the periosteum, to reduce the traumatizing effect on the periosteum. No osteoclast activity was observed in the periosteum even at day 14. However, the PDL around the moving tooth showed significant osteoclastic activity (Figure 5C).

Cortical bone resorption is followed by cortical bone formation

To investigate if osteoclast activity at the surface of cortical bone will cause the destruction of alveolar bone, micro-CT scans were completed at day 28 and 56. While at day 28, a significant decrease in bone density of buccal plate of alveolar bone was observed in comparison with sham group, at days 56 the buccal cortical plate was restored (Figure 6A).

Gene expression studies confirmed that osteoblastic activity followed the osteoclastic activity. Indeed, gene expression of early (TGF-β, ALP and Collagen) and late osteogenic markers (Osteopontin and Osteocalcin) was observed in the periosteum (Figure 6B) with peak expression at day 14 or 28 respectively.

Evaluation of the pattern of bone formation in the buccal cortical plate demonstrates that bone formation occurred along the length of the buccal cortical plate but was higher in the area of the alveolar bone crest. Biomechanical analysis took into consideration the shorter distance between point of force application and the center of resistance of the molars (shorter roots), and the spring design (Figure 6C). Due to the higher couple to force ratio that defines the type of tooth movement observed, the stress was evenly distributed at the cortical bone and the covering periosteum, however, the alveolar crest still received higher moments (Figure 6C).

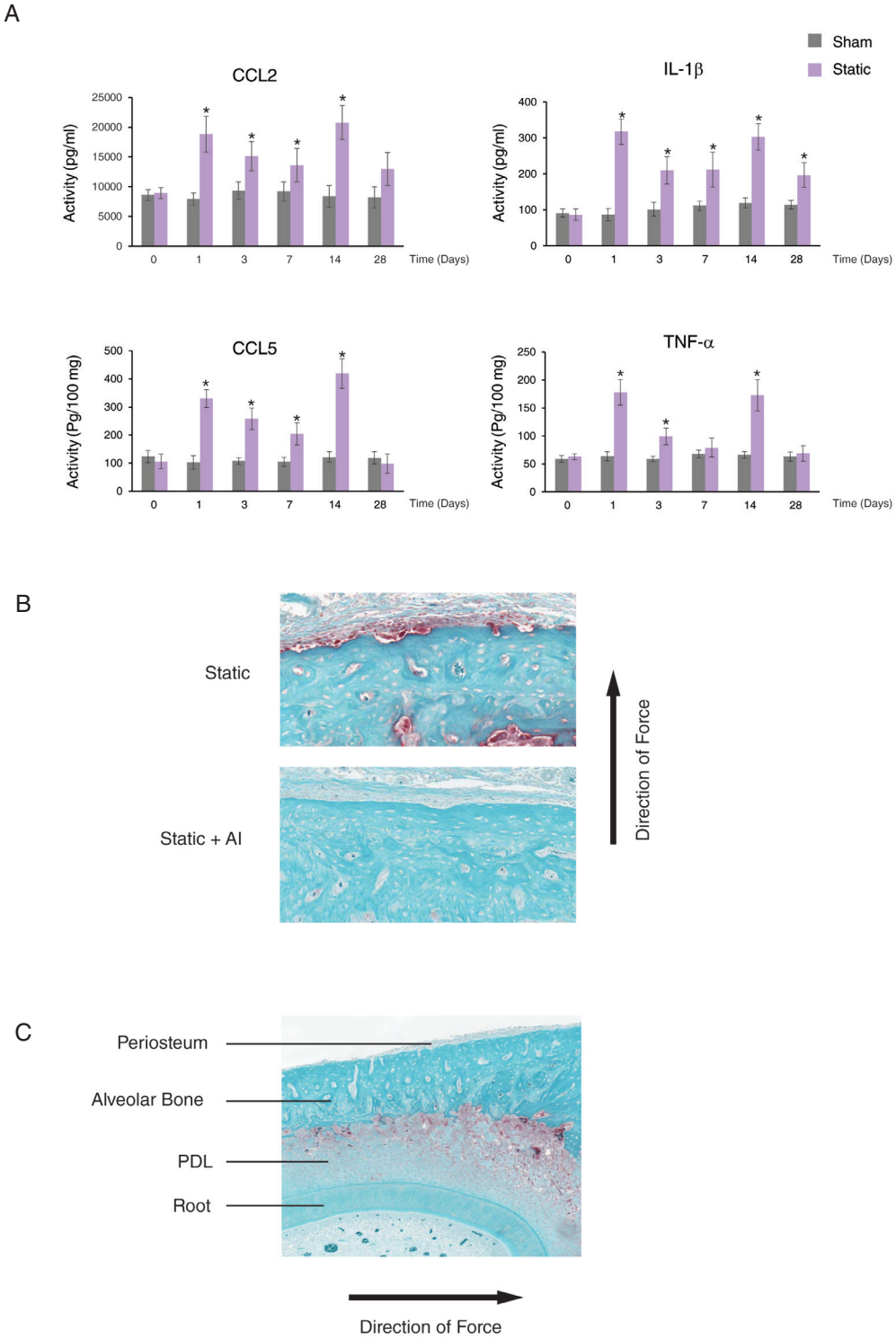

Figure 5: Static forces increase inflammatory markers in periosteum. *Mean protein concentration of IL-1α, TNF-β, CCL2, CCL5 in soft tissue (including periosteum) covering the buccal cortical plate was evaluated at different time points in periosteum by ELISA (A). Data expressed as the mean ± SD of concentration in picograms per 100 mg of tissue. Each number represents the average of 5 samples. * Static group significantly different from sham group at the same time point, p<0.05. TRAP staining of histological sections taken from buccal cortical plate of second molars in static and static plus anti-inflammatory medication after 7 days of application of static forces (B). TRAP staining of the first molar area after application of 100cN force in sagittal direction for 14 days (black arrow) (C).*

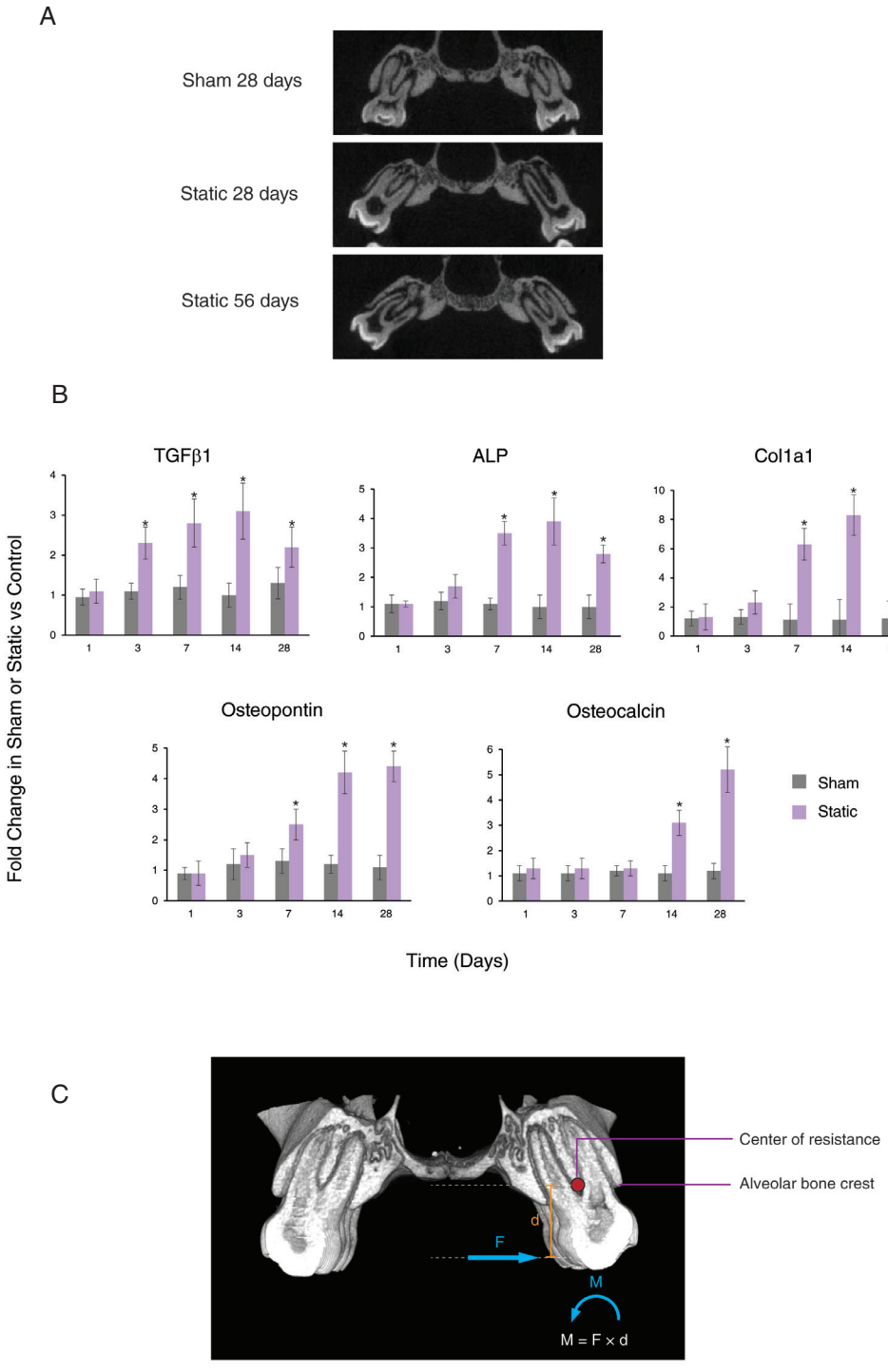

Figure 6: Static forces activate osteoblasts in periosteum resulting in bone formation. *3D micro CT reconstructed images of coronal section of maxilla at the area of second molars were compared between sham and static groups. Static group demonstrate significant decrease in bone density in area of second molars at day 28. However, after 56 days, the animals that received static force showed significant reconstruction of buccal cortical plate (A). Change in expression of osteogenic markers TGFβ1,collagen 1, ALP, Osteopontin and Osteocalcin in soft tissue covering the cortical plate of posterior teeth at different time points was measured by RT-PCR. Data are expressed as mean ± SD "fold" change in expression in comparison to control. Each value represents the average of 5 samples. * Significantly different from control group, p<0.05 (B). Schematic showing the biomechanical analysis of the force applied to the crown of the maxillary molars (C). In response to this static force (F= force), a moment will appear in the system (M = F x d, where M = moment, and d = distance between force application and center of resistance of the tooth) that produces a high stress area in the alveolar crest of the buccal cortical plate where the higher magnitude of bone formation was observed (C).*

Periosteal stimulation increases inflammation and the number of osteoclasts

Based on our biomechanical assessment showing high stress area at the buccal alveolar crest (Figure 6C), the robust bone formation in this area could be the direct response to higher moments that can result in higher activation of osteoclasts due to increased trauma to periosteum and cortical plate in this area. If the increase in bone formation in the cortical plate is osteoclast-dependent, one would expect that in the presence of the same magnitude of static forces, increasing the number of osteoclast in the area by controlled trauma to the periosteum, would stimulate further cortical bone formation.

In the next series of experiments, we induced inflammation in the periosteum by perforating attached gingiva/soft tissue covering the buccal cortical plate with small needles. First, we investigated if perforating the attached gingiva did increase the inflammatory reaction in periosteum. In response to this stimulation, the expression of different inflammatory markers increased in periosteum as show for CCL2 and IL-1β (Figure 7A). This increase was significantly higher in the group that received static force and stimulation (Static + Stim) at 1 day and 3 in comparison with the Static group (p<0.05), while the difference at other time points was not statistically significant (p>0.05) (Figure 7A). Second, we measure the expression of osteoclasts markers at different time points. Osteoclasts marker RANK, RANKL and Ctsk were significantly higher on day 1 to14 for the group that received static force and stimulation (p<0.05) (Figure 7B). Third, we evaluated the number osteoclasts in the periosteum area along the roots of the molars. We found a significant increase in the number of osteoclasts in response to the stimulation in comparison with the group that received static forces alone, on days 1, 3,7 and 14 (p< 0.05) (Figure 7C and D). These experiments together demonstrated that osteoclasts are controlled by the inflammatory reaction in the periosteum, and their numbers and activity can be increased with additional localized trauma of the periosteum.

Inflammation through osteoclast activation stimulate cortical drifting

To further evaluate the role of osteoclasts in regulating osteoblasts activity, we studied the magnitude of bone formation when osteoclast activity was boosted by stimulation of periosteum by minor trauma. We compared micro CT data from static force plus stimulation group with the sham group and with the group that only received static force. Micro CT images shows significant bone formation on the buccal cortical plate of experimental group animals (Figure 8A) 56 days after periosteal stimulation. Similarly, fluorescent microscopy of these experimental animals at day 56, demonstrates a clear increase in bone formation, that appeared as relocation of the cortical bone laterally or cortical drift (Figure 8B). To make sure this bone formation is a local effect, in another series of experiments, animals were exposed to static forces, and we stimulated the periosteum only on one side of the maxilla. Micro CT studies of these animals after 56 days demonstrate significant bone formation in the side that received stimulation (Figure 8C) which was confirmed by fluorescent microscopy (Figure 8D).

Discussion

When we study bone response to mechanical stimulation, we should differentiate between the response to static or dynamic forces. Furthermore, we should investigate what is the biological target of the mechanical stimulation. Is it the bone itself (which can be either the trabecular or cortical bone) or is the envelope that surrounds the bone, periosteum and endosteum, or both?

It has been shown that the application of bending forces to long bones can initiate the modeling machinery in the cortical plate. For example, the application of static bending forces that increase the convexity of the bone on one side and concavity on other side, was accompanied with the activation of osteoclasts on the surface of cortical bone on the convex side [29]. This phenomenon has been attributed to the direct recognition of the bending forces by the bone cells and initiation of the modeling machinery with activation of osteoclasts on the convex surface and activation of osteoblasts in concave side to resist bending [30]. Based on this proposed bone modeling process osteoblast and osteoclasts are activated separately in different surfaces, trying to reestablish the original shape of the bone.

In our experimental model, the static transverse forces that are applied perpendicular to alveolar bone have a tendency to increase the convexity of the alveolar bone especially of buccal cortical plate and the concavity of the lingual cortical plate. Similar to observations in long bones, the osteoclast appeared on the cortical buccal plate. However, when we changed the direction of force 180 degree, which supposedly should increase the convexity of the lingual cortical plate and not buccal cortical plate, osteoclasts still appeared on the buccal cortical plate, in addition to the lingual cortical plate. In both cases, the appearance of osteoclasts was a generalized phenomenon and both periosteum and endosteum were involved. This was surprising since the appearance of osteoclast was not dependent on changes in convexity of the alveolar bone, casting doubts on how the force was recognized by bone cells.

Further evaluation of the periosteum in the buccal cortical plate showed an increase of inflammatory markers in the periosteum, coinciding with the movement of the alveolar bone towards its periosteal envelope. It should be emphasized that the application of a static force to hemimaxilla is significantly different from the application of static forces to long bones. If the force can only bend the bone, the magnitude of trauma to the periosteum is much less in comparison with conditions where application of a static force, in addition to the bending effect, can also displace the bone towards its periosteal envelop. In the maxilla, due to the existence of surrounding sutures, the hemimaxilla can be displace in the direction of force. This

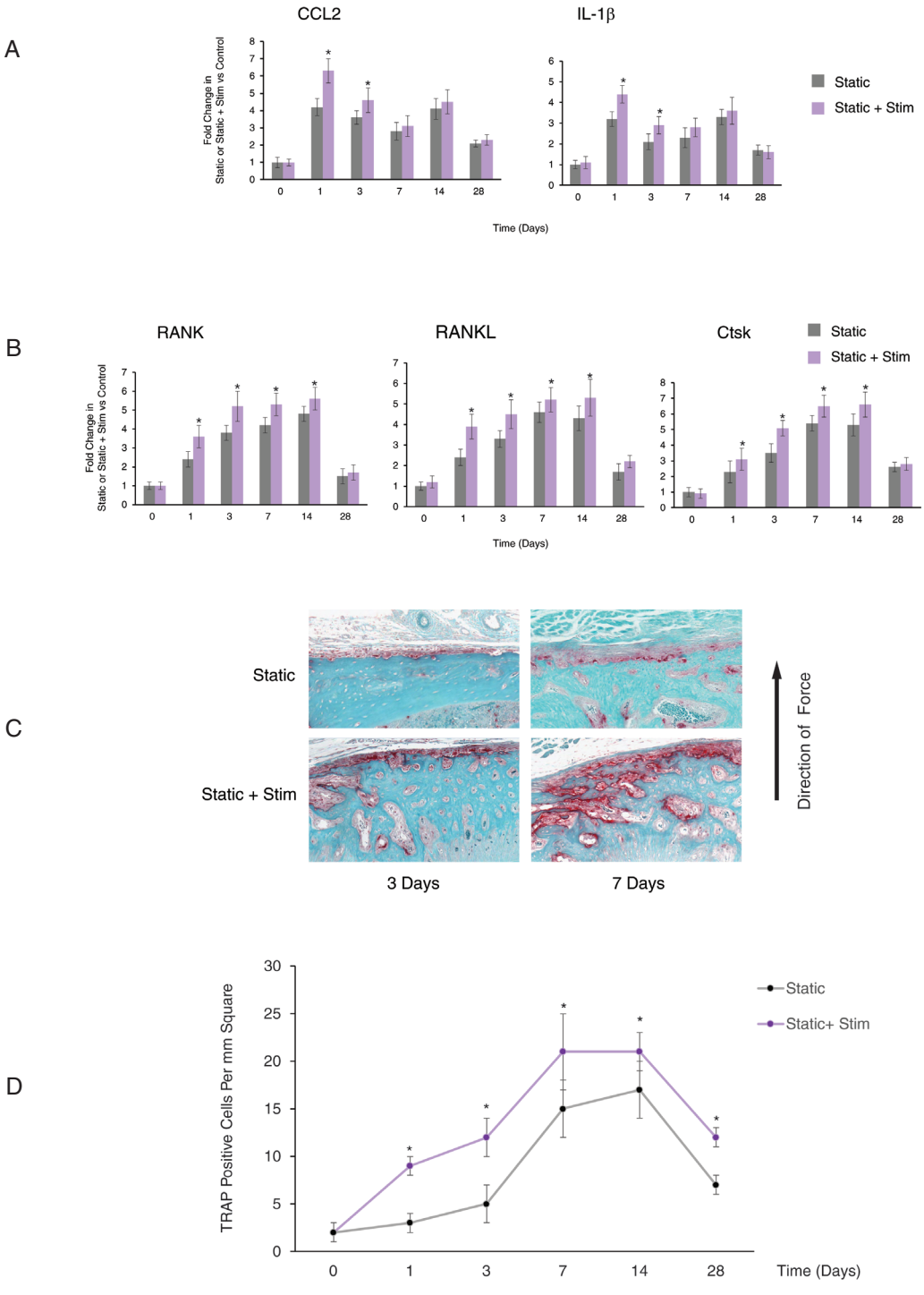

Figure 7. Periosteal Stimulation Increases inflammation and the number of TRAP-positive cells. *To study the effect of TRAP-positive cells on bone formation we increased the number of TRAP-positive cells in the periosteum by periosteal stimulation with small needles in the area of the second maxillary molar. Change in expression of CCL2, IL-1α, RANK, RANKL and Cathepsin K (Ctsk) in the soft tissue covering the cortical plate of posterior teeth was measured by RT- PCR at different time points. Data are expressed as mean ± SD "fold" change in expression in comparison to control. Each value represents the average of 5 samples. *Significantly different from static group at the same time point, p<0.05) (A and B). Immunohistochemistry for TRAP was performed in paraffin section of both "static" and "static + stim" groups to identify TRAP-positive cells in the periosteum of maxillary alveolar bone. Representative light microphotographs show TRAP-positive osteoclasts in surface of cortical bone at 3 and 7 days (C). Mean numbers of TRAP-positive cells at different time points, in the area between the mesial border of the mesial roots of the first molars and distal border of the distal roots of the second molars. Each value represents the mean ± SD of five animals. * Significantly different from control, p<0.05 (D).*

movement follows the pattern of the opening of the suture as we have previously demonstrated [26, 31]. The outcome of this movement is the increase in the width of the palate. In the current experiments, the inflammatory markers peaked at the time this movement was maximum. This observation suggests that the periosteum is traumatized by the displacement of the alveolar bone.

In this article, we refer to the TRAP positive cells that appeared in periosteum as osteoclasts since traditionally they are considered mostly bone resorbing cells. However, many have referred to these cells as osteo-macrophages, a subgroup of macrophages that reside in the periosteum and originate from a myeloid lineage. These can be mono-nuclear and play a more complex role in the periosteum homeostasis [32-36]. These cells also have the ability to directly sense the mechanical stimulation however, this mechanism is perhaps more relevant in response to dynamic forces [37, 38].

Here, we demonstrated that static forces applied to the cortical bone can stimulate osteoclasts in the periosteum through an inflammatory reaction. The reaction of the periosteum in these experiments was similar to the reaction of the periodontal ligament during orthodontic tooth movement when static orthodontic forces stimulate osteoclasts recruitment and activity all around the roots of the moving tooth [39]. Similar to what we observed in our tooth movement model, the presence of these cells in the periosteum could be inhibited by anti-inflammatory drugs.

To further investigate the role of trauma to the periosteum,

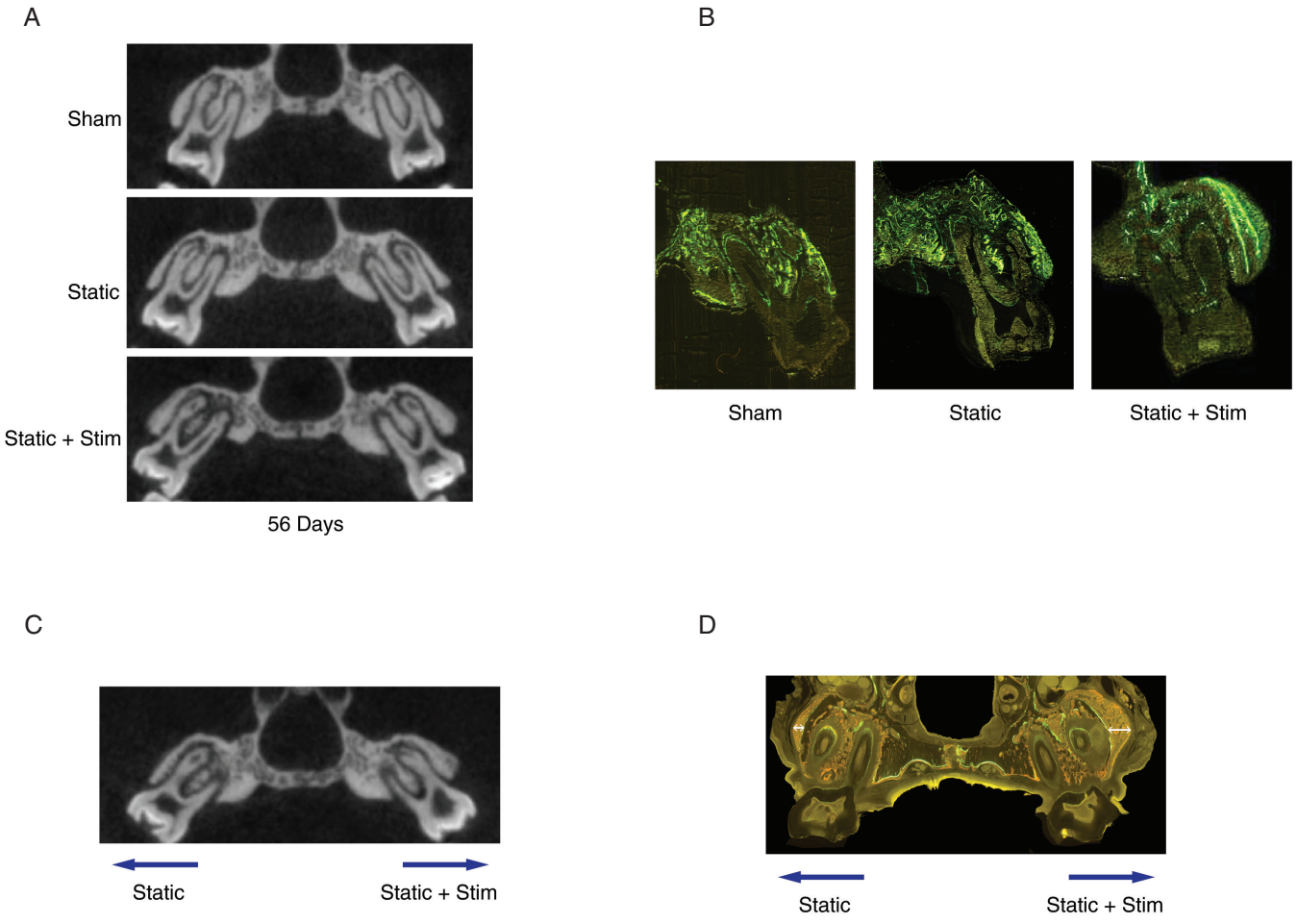

Figure 8: Cortical bone formation was dependent on osteoclast activation in the periosteum. *Osteoclasts activity was increased by bilateral application of periosteal stimulation in the area of the second molars and the effect on bone formation was compared by microCT images of coronal sections of maxilla in the area of second molars at day 56. Sections of Sham, Static and Static + Stim are shown 56 days after stimulation (A). Fluorescent microscopy images of coronal section of maxilla of Sham, Static, or Static + Stim at the area of second molars at day 56 are shown (B). Bone labeling was performed by Calcein green on day 0, 28 and 54. Micro CT images of mid-coronal section of maxilla at the area of second molars in animals that received static force in the maxilla and stimulation only in one side show asymmetrical bone formation (C). Fluorescent microscopy images of mid-coronal section of maxilla of animals that received static and unilateral periosteal stimulation in the area of second molars at day 56 (D). Bone labeling was performed by Calcein on days 0 (Green), and Xylenol Orange at day 26 and 54 (Orange). White arrows mark the change in the width of the cortical bone over the second molar area.*

caused by maxillary displacement, in the appearance of osteoclasts we changed the direction of force from perpendicular to parallel to the periosteum, and noticed that there was no significant stimulation of osteoclasts in the periosteum. This lack of response could be due to lack of movement of the bone towards or away from periosteum.

Since the static transverse forces in our model were applied through the teeth to the alveolar bone, we investigated if this phenomenon was related to the teeth moving. It has been assumed that movement of the tooth toward buccal cortical plate, will push the tooth out of alveolar bone and cause resorption of the buccal cortical plate [40, 41]. However, our observations reject this hypothesis because osteoclasts appearance occurred much earlier than tooth movement and even occurred in the area of the maxilla where there were no teeth. Furthermore, in none of our samples did the teeth reached to buccal cortical plate in 28 days.

Next, we evaluated if the cortical bone would be restored after static force application, osteoclast activation, and bone resorption. As expected, osteoblasts were indeed activated after a delay, and created a new buccal cortical plate. This new cortical plate, in comparison with the original position of the buccal cortical plate, showed a lateral drift and an increase in size, with no loss of cortical bone in its horizontal or vertical dimensions. This phenomenon is similar to bone formation observed during chronic pathologies such as cysts and tumors [21-23].

Two different bone movements should be identified in these studies. One, is the displacement of the cortical plate laterally due to movement of the hemi-maxilla in the same direction of the static force which occurs after opening of the sutures. This is accompanied by an increase in the width of the palate observed in a cross-section of alveolar bone and palate. This movement is not considered cortical drifting. Second, is the drift of the cortical bone laterally that can be observed in the fluorescent microscopy images. This cortical drifting was not observed in the first month after application of static forces, but was visible on second month, which argues that bone formation on the cortical plate is a delayed phenomenon. This observation has two new important clinical applications. First, the buccal cortical plate can go through significant drifting and is not a fix boundary of the jaws as previously believed. Second, the formation of a new buccal cortical plate is a delayed reaction, and perhaps the clinical radiographic evaluation of this bone should not be completed right after application of static forces but, especially in humans, should be evaluated months after application of the force. It is logical to assume that if the formation of cortical bone is a delayed reaction, then the area should not be disturbed surgically during this phase of modelling.

Evaluation of the microCT and fluorescent microscopy images in the frontal view, shows that bone formation was distributed almost evenly along the buccal surface of cortical bone, with slightly more activity around the alveolar bone crest. This can be explained by the mechanical design and the shorter root of molars in the rat that allowed an even force distribution on the alveolar bone, with concentration of stresses on the alveolar bone crest due to slight tilting of the teeth. Therefore, additional trauma and activation of osteoclasts on the alveolar bone crest may explain the further bone formation that is observed in this area.

To further demonstrate that bone formation in the periosteum was related to osteoclasts activity, we increased the number of osteoclasts at the surface of bone by direct trauma to the periosteum. This is important since while we show that static forces produced by displacement of bone can traumatize the periosteum and stimulate osteoclast activity, we did not explain how bone formation in response to the static forces occurred.

Previous studies demonstrated that osteoclasts can recruit the osteoblasts to the bone surface and increase bone formation by secreting different factors such as TGFβ1 [32, 42-47]. Furthermore, our findings are in agreement with studies that showed that the adaptation of cortical bone to mechanical stimulation originates from periosteum [42, 48-50]. However, in previous studies, the mechanical stimulation was dynamic, while in our studies, we focused mostly on static forces, which had not been studied before.

Our study can explain previous observations that suggest that periosteum plays a significant role in the growth of the cortical bone [51-54]. Forces produced by growth are partly static forces due to increases in the mass of soft tissues, changes in the rest position of muscles, or many other examples, and partly dynamic forces due to increase in magnitude of forces of muscles during function. In this study we did not investigate the effect of dynamic forces on periosteum but, we demonstrated that the static forces, as long as they are applied slowly, can have an osteogenic effect on cortical bone, a mechanism that perhaps is used during growth of bone, regardless if it is physiological or pathological growth. It is interesting to mention that a similar mechanism has been observed during endochondral bone growth, where periosteum and perichondrium interact with cartilage and affect the cartilage growth [55, 56].

Cortical drifting has been reported during growth of the skeleton, while different patterns of osteoclast and osteoblast activity has been described on different surfaces of cortical bone [57]. Since muscles and soft tissue are connected to bone through sharpy fibers [58] crossing the periosteum to the bone, one cannot help but to think that an increase in size and function of soft tissue, perhaps by increasing the magnitude of static and dynamic forces on the surface of the bone, increase insult on the periosteum and therefore stimulate bone formation. This is very important clinically, as it provides evidence supporting the hypothesis that growth of cortical bone depends on the growth of soft tissues [59-61]. More studies in this area are necessary to further understand this important phenomenon.

While due to the limited length of our study we were not able to investigate the long term changes in the shape of the alveolar bone, we believe that the changes in morphology

of bone occurring during application of static forces and periosteum remodeling, should be maintained afterwards by normal function of muscles and jaw activity. In presence of normal function, the bone restores its original shape as has been observed during fracture healing of long bones [62]. In absence of supporting function, there is no need for the body to maintain the new bone. Therefore, we hypothesize that periosteal stimulation and cortical bone formation may result is stable new bone formation, when accompanied with proper change in function. At this moment we do not have enough data to support this view.

Understanding the mechanism of periosteal stimulation during application of static forces also can explain the mechanism of bone formation during distraction osteogenesis where periosteum is exposed to relatively static forces [63].

Our research demonstrates how both dynamic and static forces by influencing different targets can reshape the cortical form [2]. Cortical bone is the main factor in sculpturing the general form of our skeleton. Therefore, different disciplines of science, when studying the form of the skeleton should pay attention to not only to dynamic forces and their direct effect on bone, but should consider static forces that indirectly affect the cortical bone and therefore our form.

Conclusion

In conclusion, while osteocytes and periosteum osteoclasts/macrophages can play a significant role in recognizing dynamic mechanical stimulation directly and initiate mechanical adaptation of the skeleton, inflammation based activation of osteoclasts/macrophages play a significant role in the response of cortical bone to static forces. In both cases, periosteum contains all the required progenitor cells to allow these mechanical bone adaptions. This study demonstrates that cortical plate of the alveolar bone can be remodeled in adult rats in response to the static forces. Static forces induce a transient inflammatory reaction in the periosteum, followed by activation of osteoclasts and later of osteoblasts that restore the cortical bone. The following observations have significant clinical importance:

1. Activation of osteoclasts occurred independent of magnitude of tooth movement.
2. Resorption of cortical bone and rebuilding of its surface resulted in lateral movement of the cortical bone in space, referred to as cortical drifting.
3. Bone formation is a delayed phenomenon. In humans, perhaps this phenomenon may occur even later. Clinicians should recognize this phenomena and refrain from disturbing the process with any procedures that can affect the periosteum.
4. Periosteal stimulation can be used to induce cortical drifting and reshaping the alveolar cortical plate

Innovation

There are two main aspects to the innovations discussed in this article. First, we propose a new mechanism for how bones respond to static force, and their mechanism of adaptation, suggesting a role for cortical drifting during growth and the creation of our final skeletal form. Second, this study demonstrates for the first time how periosteal stimulation (using small needles) amplifies the bone formation at the surface of the cortical bone and can be used to promote cortical drifting and reshaping of the cortical bone. Being able to control cortical drift can have a significantly impact in clinical orthodontic and dentofacial orthopedics by allowing corrections of severe deformities without need for maxillofacial surgery.

Acknowledgment

We would like to take this opportunity and thank the following individuals for their contribution to different aspects of this project: Mohammad Hamidaddin, Chris Teo, Sarah Alansari, and Kanwipa Poorisat.

References

1. Rubin C, Turner AS, Bain S, Mallinckrodt C, McLeod K. Anabolism. Low mechanical signals strengthen long bones. Nature. 2001;412(6847):603-4. doi: 10.1038/35088122. PubMed PMID: 11493908.

2. Alikhani M, Khoo E, Alyami B, Raptis M, Salgueiro JM, Oliveira SM, et al. Osteogenic effect of high-frequency acceleration on alveolar bone. J Dent Res. 2012;91(4):413-9. Epub 20120214. doi: 10.1177/0022034512438590. PubMed PMID: 22337699; PubMed Central PMCID: PMCPMC3310758.

3. Frost HM. Wolff's Law and bone's structural adaptations to mechanical usage: an overview for clinicians. Angle Orthod. 1994;64(3):175-88. doi: 10.1043/0003-3219(1994)064<0175:Wlabsa>2.0.Co;2. PubMed PMID: 8060014.

4. Sugiyama T, Price JS, Lanyon LE. Functional adaptation to mechanical loading in both cortical and cancellous bone is controlled locally and is confined to the loaded bones. Bone. 2010;46(2):314-21. doi: https://doi.org/10.1016/j.bone.2009.08.054.

5. Tomlinson RE, Li Z, Li Z, Minichiello L, Riddle RC, Venkatesan A, et al. NGF-TrkA signaling in sensory nerves is required for skeletal adaptation to mechanical loads in mice. Proc Natl Acad Sci U S A. 2017;114(18):E3632-e41. Epub 20170417. doi: 10.1073/pnas.1701054114. PubMed PMID: 28416686; PubMed Central PMCID: PMCPMC5422802.

6. Brodt MD, Silva MJ. Aged mice have enhanced endocortical response and normal periosteal response compared with young-adult mice following 1 week of axial tibial compression. J Bone Miner Res. 2010;25(9):2006-15. doi: 10.1002/jbmr.96. PubMed PMID: 20499381; PubMed Central PMCID: PMCPMC3153404.

7. Johannesdottir F, Thrall E, Muller J, Keaveny TM, Kopperdahl DL, Bouxsein ML. Comparison of non-invasive assessments of strength of the proximal femur. Bone. 2017;105:93-102. Epub 20170721. doi: 10.1016/j.bone.2017.07.023. PubMed PMID: 28739416.

8. Alikhani M, Lopez JA, Alabdullah H, Vongthongleur T, Sangsuwon C, Alikhani M, et al. High-Frequency Acceleration: Therapeutic Tool to Preserve Bone following Tooth Extractions. J Dent Res. 2016;95(3):311-8. Epub 20151215. doi: 10.1177/0022034515621495. PubMed PMID: 26672126;

PubMed Central PMCID: PMCPMC6728694.

9. Srinivasan S, Balsiger D, Huber P, Ausk BJ, Bain SD, Gardiner EM, et al. Static Preload Inhibits Loading-Induced Bone Formation. JBMR Plus. 2019;3(5):e10087. Epub 20181011. doi: 10.1002/jbm4.10087. PubMed PMID: 31131340; PubMed Central PMCID: PMCPMC6524670.
10. Kazakia GJ, Tjong W, Nirody JA, Burghardt AJ, Carballido-Gamio J, Patsch JM, et al. The influence of disuse on bone microstructure and mechanics assessed by HR-pQCT. Bone. 2014;63:132-40. Epub 20140303. doi: 10.1016/j.bone.2014.02.014. PubMed PMID: 24603002; PubMed Central PMCID: PMCPMC4041600.

11. Schätzle M, Männchen R, Zwahlen M, Lang NP. Survival and failure rates of orthodontic temporary anchorage devices: a systematic review. Clin Oral Implants Res. 2009;20(12):1351-9. Epub 20090930. doi: 10.1111/j.1600-0501.2009.01754.x. PubMed PMID: 19793320.

12. Rubin CT, Lanyon LE. Regulation of bone mass by mechanical strain magnitude. Calcif Tissue Int. 1985;37(4):411-7. doi: 10.1007/bf02553711. PubMed PMID: 3930039.

13. Pollack SR, Salzstein R, Pienkowski D. Streaming potentials in fluid-filled bone. Ferroelectrics. 1984;60(1):297-309. doi: 10.1080/00150198408017530.
14. Weinbaum S, Cowin SC, Zeng Y. A model for the excitation of osteocytes by mechanical loading-induced bone fluid shear stresses. J Biomech. 1994;27(3):339-60. doi: 10.1016/0021-9290(94)90010-8. PubMed PMID: 8051194.

15. Oxlund BS, Ørtoft G, Andreassen TT, Oxlund H. Low-intensity, high-frequency vibration appears to prevent the decrease in strength of the femur and tibia associated with ovariectomy of adult rats. Bone. 2003;32(1):69-77. doi: 10.1016/s8756-3282(02)00916-x. PubMed PMID: 12584038.

16. Qin YX, Kaplan T, Saldanha A, Rubin C. Fluid pressure gradients, arising from oscillations in intramedullary pressure, is correlated with the formation of bone and inhibition of intracortical porosity. J Biomech. 2003;36(10):1427-37. doi: 10.1016/s0021-9290(03)00127-1. PubMed PMID: 14499292.

17. Malone AM, Batra NN, Shivaram G, Kwon RY, You L, Kim CH, et al. The role of actin cytoskeleton in oscillatory fluid flow-induced signaling in MC3T3-E1 osteoblasts. Am J Physiol Cell Physiol. 2007;292(5):C1830-6. Epub 20070124. doi: 10.1152/ajpcell.00352.2005. PubMed PMID: 17251324; PubMed Central PMCID: PMCPMC3057612.

18. Garman R, Gaudette G, Donahue LR, Rubin C, Judex S. Low-level accelerations applied in the absence of weight bearing can enhance trabecular bone formation. J Orthop Res. 2007;25(6):732-40. doi: 10.1002/jor.20354. PubMed PMID: 17318899.

19. Robling AG, Turner CH. Mechanical signaling for bone modeling and remodeling. Crit Rev Eukaryot Gene Expr. 2009;19(4):319-38. doi: 10.1615/critreveukargeneexpr.v19.i4.50. PubMed PMID: 19817708; PubMed Central PMCID: PMCPMC3743123.

20. Robling AG, Duijvelaar KM, Geevers JV, Ohashi N, Turner CH. Modulation of appositional and longitudinal bone growth in the rat ulna by applied static and dynamic force. Bone. 2001;29(2):105-13. doi: 10.1016/s8756-3282(01)00488-4. PubMed PMID: 11502470.

21. Waldman S, Shimonov M, Yang N, Spielman D, Godfrey KJ, Dean KE, et al. Benign bony tumors of the paranasal sinuses, orbit, and skull base. American Journal of Otolaryngology. 2022;43(3):103404. doi: https://doi.org/10.1016/j.amjoto.2022.103404.

22. Sarrafpour B, El-Bacha C, Li Q, Zoellner H. Roles of functional strain and capsule compression on mandibular cyst expansion and cortication. Archives of Oral Biology. 2019;98:1-8. doi: https://doi.org/10.1016/j.archoralbio.2018.10.035.

23. High AS, Hirschmann PN. Symptomatic residual radicular cysts. J Oral Pathol. 1988;17(2):70-2. doi: 10.1111/j.1600-0714.1988.tb01509.x. PubMed PMID: 3134534.

24. Raab-Cullen DM, Akhter MP, Kimmel DB, Recker RR. Bone response to alternate-day mechanical loading of the rat tibia. J Bone Miner Res. 1994;9(2):203-11. doi: 10.1002/jbmr.5650090209. PubMed PMID: 8140933.

25. Meade JB, Cowin SC, Klawitter JJ, Van Buskirk WC, Skinner HB. Bone remodeling due to continuously applied loads. Calcified Tissue International. 1984;36(1):S25-S30. doi: 10.1007/BF02406130.

26. Mani Alikhani SA, Mohammed M Al Jearah , Niraj Gadhavi, Mohammad A Hamidaddin, Fadwa A Shembesh, Chinapa Sangsuwon, Jeanne M Nervina, Cristina C Teixeira. Osteoclasts: the biological knife in sutural responses to mechanical stimulation. Innovation. 2018;1(4):e1. doi: https://doi.org/10.30771/2018.3.

27. Cox PG, Rayfield EJ, Fagan MJ, Herrel A, Pataky TC, Jeffery N. Functional evolution of the feeding system in rodents. PLoS One. 2012;7(4):e36299. Epub 2012/05/05. doi: 10.1371/journal.pone.0036299. PubMed PMID: 22558427; PubMed Central PMCID: PMCPMC3338682.

28. Erben RG. Embedding of bone samples in methylmethacrylate: an improved method suitable for bone histomorphometry, histochemistry, and immunohistochemistry. J Histochem Cytochem. 1997;45(2):307-13. Epub 1997/02/01. PubMed PMID: 9016319.

29. Frost HM. Skeletal structural adaptations to mechanical usage (SATMU): 1. Redefining Wolff's law: the bone modeling problem. Anat Rec. 1990;226(4):403-13. doi: 10.1002/ar.1092260402. PubMed PMID: 2184695.

30. Frost HM. Mechanical determinants of bone modeling. Metab Bone Dis Relat Res. 1982;4(4):217-29. doi: 10.1016/0221-8747(82)90031-5. PubMed PMID: 6763662.

31. Alikhani M, Alansari S, Al Jearah MM, Gadhavi N, Hamidaddin MA, Shembesh FA, et al. Biphasic sutural response is key to palatal expansion. Journal of the World Federation of Orthodontists. 2019;8(1):9-17. doi: 10.1016/j.ejwf.2019.01.002.

32. Deng R, Li C, Wang X, Chang L, Ni S, Zhang W, et al. Periosteal CD68(+) F4/80(+) Macrophages Are Mechanosensitive for Cortical Bone Formation by Secretion and Activation of TGF-β1. Adv Sci (Weinh). 2022;9(3):e2103343. Epub 20211202. doi: 10.1002/advs.202103343. PubMed PMID: 34854257; PubMed Central PMCID: PMCPMC8787385.

33. Vi L, Baht GS, Soderblom EJ, Whetstone H, Wei Q, Furman B, et al. Macrophage cells secrete factors including LRP1 that orchestrate the rejuvenation of bone repair in mice. Nature Communications. 2018;9(1):5191. doi: 10.1038/s41467-018-07666-0.

34. Davies LC, Jenkins SJ, Allen JE, Taylor PR. Tissue-resident macrophages. Nature Immunology. 2013;14(10):986-95. doi: 10.1038/ni.2705.

35. Biswas SK, Mantovani A. Orchestration of metabolism by macrophages. Cell Metab. 2012;15(4):432-7. doi: 10.1016/j.cmet.2011.11.013. PubMed PMID: 22482726.

36. Allen MR, Hock JM, Burr DB. Periosteum: biology, regulation, and response to osteoporosis therapies. Bone. 2004;35(5):1003-12. doi: 10.1016/j.bone.2004.07.014. PubMed PMID: 15542024.

37. Kao C-T, Huang T-H, Fang H-Y, Chen Y-W, Chien C-F, Shie M-Y, et al. Tensile force on human macrophage cells promotes osteoclastogenesis through receptor activator of nuclear factor κB ligand induction. Journal of Bone and Mineral Metabolism. 2016;34(4):406-16. doi: 10.1007/s00774-015-0690-2.

38. Solis AG, Bielecki P, Steach HR, Sharma L, Harman CCD, Yun S, et al. Mechanosensation of cyclical force by PIEZO1 is essential for innate immunity. Nature. 2019;573(7772):69-74. doi: 10.1038/s41586-019-1485-8.

39. Teixeira CC, Khoo E, Tran J, Chartres I, Liu Y, Thant LM, et al. Cytokine expression and accelerated tooth movement. J Dent Res. 2010;89(10):1135-41. Epub 20100716. doi: 10.1177/0022034510373764. PubMed PMID: 20639508; PubMed Central PMCID: PMCPMC3318047.

40. Cardinal L, da Rosa Zimermann G, Mendes FM, Andrade I, Jr., Oliveira DD, Dominguez GC. Dehiscence and buccal bone thickness after rapid maxillary expansion in young patients with unilateral cleft lip and palate. Am J Orthod Dentofacial Orthop. 2022;162(1):16-23. Epub 20220210. doi: 10.1016/j.ajodo.2021.01.038. PubMed PMID: 35153114.

41. Lin L, Ahn HW, Kim SJ, Moon SC, Kim SH, Nelson G. Tooth-borne vs bone-borne rapid maxillary expanders in late adolescence. Angle Orthod. 2015;85(2):253-62. Epub 20141209. doi: 10.2319/030514-156.1. PubMed PMID: 25490552; PubMed Central PMCID: PMCPMC8631879.

42. Gao B, Deng R, Chai Y, Chen H, Hu B, Wang X, et al. Macrophage-lineage TRAP+ cells recruit periosteum-derived cells for periosteal osteogenesis and regeneration. J Clin Invest. 2019;129(6):2578-94. Epub 20190404. doi: 10.1172/jci98857. PubMed PMID: 30946695; PubMed Central PMCID: PMCPMC6538344.

43. Cho SW, Soki FN, Koh AJ, Eber MR, Entezami P, Park SI, et al. Osteal macrophages support physiologic skeletal remodeling and anabolic actions of parathyroid hormone in bone. Proc Natl Acad Sci U S A. 2014;111(4):1545-50. Epub 20140109. doi: 10.1073/pnas.1315153111. PubMed PMID: 24406853; PubMed Central PMCID: PMCPMC3910564.

44. Chang MK, Raggatt LJ, Alexander KA, Kuliwaba JS, Fazzalari NL, Schroder K, et al. Osteal tissue macrophages are intercalated throughout human and mouse bone lining tissues and regulate osteoblast function in vitro and in vivo. J Immunol. 2008;181(2):1232-44. doi: 10.4049/jimmunol.181.2.1232. PubMed PMID: 18606677.

45. Sinder BP, Pettit AR, McCauley LK. Macrophages: Their Emerging Roles in Bone. J Bone Miner Res. 2015;30(12):2140-9. doi: 10.1002/jbmr.2735. PubMed PMID: 26531055; PubMed Central PMCID: PMCPMC4876707.

46. Vi L, Baht GS, Whetstone H, Ng A, Wei Q, Poon R, et al. Macrophages promote osteoblastic differentiation in-vivo: implications in fracture repair and bone homeostasis. J Bone Miner Res. 2015;30(6):1090-102. doi: 10.1002/jbmr.2422. PubMed PMID: 25487241.

47. Wang B, Pourshafeie A, Zitnik M, Zhu J, Bustamante CD, Batzoglou S, et al. Network enhancement as a general method to denoise weighted biological networks. Nature Communications. 2018;9(1):3108. doi: 10.1038/s41467-018-05469-x.

48. Debnath S, Yallowitz AR, McCormick J, Lalani S, Zhang T, Xu R, et al. Discovery of a periosteal stem cell mediating intramembranous bone formation. Nature. 2018;562(7725):133-9. doi: 10.1038/s41586-018-0554-8.

49. Duchamp de Lageneste O, Julien A, Abou-Khalil R, Frangi G, Carvalho C, Cagnard N, et al. Periosteum contains skeletal stem cells with high bone regenerative potential controlled by Periostin. Nature Communications. 2018;9(1):773. doi: 10.1038/s41467-018-03124-z.

50. Zannit HM, Silva MJ. Proliferation and Activation of Osterix-Lineage Cells Contribute to Loading-Induced Periosteal Bone Formation in Mice. JBMR Plus. 2019;3(11):e10227. Epub 20190911. doi: 10.1002/jbm4.10227. PubMed PMID: 31768488; PubMed Central PMCID: PMCPMC6874181.

51. Foolen J, van Donkelaar CC, Ito K. Intracellular tension in periosteum/perichondrium cells regulates long bone growth. J Orthop Res. 2011;29(1):84-91. doi: 10.1002/jor.21224. PubMed PMID: 20690184.

52. Gigante A, Chillemi C, Quaglino D, Miselli M, Pasquali-Ronchetti I. DL-penicillamine induced alteration of elastic fibers of periosteum-perichondrium and associated growth inhibition: an experimental study. J Orthop Res. 2001;19(3):398-404. doi: 10.1016/s0736-0266(00)90033-0. PubMed PMID: 11398852.

53. Schumacher B, Albrechtsen J, Albrechtsen J, Keller J, Flyvbjerg A, Hvid I. Periosteal insulin-like growth factor I and bone formation Changes during tibial lengthening in rabbits. Acta Orthopaedica Scandinavica. 1996;67(3):237-41. doi: 10.3109/17453679608994679.

54. Kuijpers-Jagtman AM, Bex JH, Maltha JC, Daggers JG. Longitudinal growth of the rabbit femur after vascular and periosteal interference. Anat Anz. 1988;167(5):349-58. PubMed PMID: 3232844.

55. Bertram JEA, Polevoy Y, Cullinane DM. Mechanics of Avian Fibrous Periosteum: Tensile and Adhesion Properties During Growth. Bone. 1998;22(6):669-75. doi: https://doi.org/10.1016/S8756-3282(98)00035-0.

56. Crilly RG. Longitudinal overgrowth of chicken radius. J Anat. 1972;112(Pt 1):11-8. PubMed PMID: 5086208; PubMed Central PMCID: PMCPMC1271338.

57. Enlow DH, Moyers RE, Merow WW. Handbook of Facial Growth: Saunders; 1982.

58. Evans SF, Chang H, Knothe Tate ML. Elucidating multiscale periosteal mechanobiology: a key to unlocking the smart properties and regenerative capacity of the periosteum? Tissue Eng Part B Rev. 2013;19(2):147-59. Epub 20130201. doi: 10.1089/ten.TEB.2012.0216. PubMed PMID: 23189933; PubMed Central PMCID: PMCPMC3589889.

59. Bromage TG. The Functional Matrix Hypothesis Revisited. 5. Orofacial Capsular Matrices Defined. Innovation. 2022.

60. Botzenhart UU, Keil C, Tsagkari E, Zeidler-Rentzsch I, Gredes T, Gedrange T. Influence of botulinum toxin A on craniofacial morphology after injection into the right masseter muscle of dystrophin deficient (mdx-) mice. Annals of Anatomy - Anatomischer Anzeiger. 2021;236:151715. doi: https://doi.org/10.1016/j.aanat.2021.151715.

61. Moss-Salentijn L. Melvin L. Moss and the functional matrix. J Dent Res. 1997;76(12):1814-7. doi: 10.1177/00220345970760120201. PubMed PMID: 9390473.

62. Egawa S, Miura S, Yokoyama H, Endo T, Tamura K. Growth and differentiation of a long bone in limb development, repair and regeneration. Dev Growth Differ. 2014;56(5):410-24. Epub 20140523. doi: 10.1111/dgd.12136. PubMed PMID: 24860986.

63. Kadlub N, Dallard J, Kogane N, Galliani E, Boisson J. Mandibular magnetic distractor: preclinical validation. British Journal of Oral and Maxillofacial Surgery. 2022;60(6):767-72. doi: https://doi.org/10.1016/j.bjoms.2021.11.008.